Energy 88 (2015) 93–100

Contents lists available at ScienceDirect

Energy

journal homepage: www.elsevier.com/locate/energy

Performance of ammonia–water based cycles for power generation from low enthalpy heat sources

Hanna Mergner [a, *], Thomas Weimer [b]

[a] EnBW Energie Baden-Württemberg AG, Karlsruhe, Germany
[b] Makatec GmbH, Bondorf, Germany

ARTICLE INFO

Article history:
Received 31 October 2014
Received in revised form
15 April 2015
Accepted 16 April 2015
Available online 26 May 2015

Keywords:
Ammonia cycle
ORC
Geothermal power
Kalina
Low temperature energy sources

ABSTRACT

Cost efficient power generation from low temperature heat sources requires an optimal usage of the available heat. In addition to the ORC (Organic Rankine Cycles), cycles with ammonia and water as working fluid show promising results regarding efficiency. Due to their non-isothermal phase change, mixtures can adapt well to a liquid heat source temperature profile and reduce the exergetic losses. In this analysis thermodynamic calculations on the layouts of two existing ammonia–water cycles are compared: a geothermal power plant based on a Siemens' patent and a modified lab plant based on a patent invented by Kalina (KCS-34). The difference between the two cycles is the position of the internal heat recovery. Cycle simulations were carried out at defined boundary conditions in order to identify optimal operation parameters. For the selected heat source of 393.15 K (hot water) the ammonia mass fraction between 80% and 90% results in the best performance in both configurations. In general, the layout of Siemens achieves a slightly better efficiency compared to the KCS-34. Compared to an ORC using R245fa as working fluid, the exergetic efficiency can be increased by the ammonia/water based cycles by approximately 25%.

1. Introduction

Power generation from low temperature heat sources including geothermal heat or waste heat from processing industries typically yields rather low energy efficiency. The efficiency of a thermal power cycle is mainly determined by the temperature difference between the heat source and the heat sink. In order to generate power with low enthalpy cycles more efficiently, the exergetic losses during the heat transfer must be minimized. Besides the well-known Organic Rankine Cycle (ORC), a similar cycle, the so-called "Kalina Cycle" is used as binary cycle.

Several literature sources see the Kalina Cycle as a promising cycle for increasing the power output efficiency of low temperature heat source based cycles [1–5]. The working fluid of the Kalina Cycle is a zeotropic mixture, usually a mixture of ammonia (NH_3) and water (H_2O). The use of such a mixture leads to a sliding temperature during isobaric evaporation and condensation and appears to adapt better to single phase heat sources (industrial waste heat, geothermal heat, biomass heat) and heat sinks.

The Kalina cycle is named after Dr. Alexander Kalina who invented it [6]. Since 1982 Kalina patents his inventions on a variety of embodiments of thermal cycles for different temperature applications varying from rather simple systems to very complex and more expensive systems [7].

Until today, only few cycles have been realized. Among the first projects are a demonstration plant (Canoga park) in the USA and two waste heat recovery Kalina plants in Japan [1]. In Europe, three Kalina cycles using geothermal heat for power generation exist as of today (2015) to the knowledge of the authors. The first one is a Kalina plant in Húsavík, Iceland. This 2 MW plant is based on the Kalina cycle system called KCS-34 that was published in a European patent application by Kalina in 2001 [8]. In this patent, four different embodiments are described. The Húsavík plant presents case three, which is a simplified embodiment with no extracted stream [9]. The other two are located in Germany, in Unterhaching and Bruchsal, both of which have been built by Siemens from 2007 to 2009 [10,11]. Their cycle layout is very similar to the simplest embodiment of KCS-34. The layout of this cycle differs from the original KCS-34 by the internal heat exchangers and was published

* Corresponding author.
E-mail addresses: h.mergner@enbw.com (H. Mergner), gomma@champresso.de (T. Weimer).

http://dx.doi.org/10.1016/j.energy.2015.04.084
0360-5442/

in a patent by Siemens in 2006 [12]. In some articles this cycle is be referred to as Kalina SG-1 [13]. Thus, the cycle is called "KC SG1" in this paper. While the Siemens configuration recovers heat from the expanded steam and the bypassed liquid, the KSC-34 only utilizes the bypassed liquid. According to [12], the mechanical and electrical energy output can be increased slightly compared to the KSC-34. Besides the existing patent no published information can be found regarding the performance of the Kalina cycle implemented in Bruchsal and Unterhaching compared to the simplified KSC-34. The KSC-34 is not only applied for applications of power generation, but can also be used in a modified configuration as absorption/desorption refrigeration process. An existing lab plant is operated by Makatec. The difference compared to the existing Kalina plants is the concentration of NH_3. The power plant in Bruchsal operates with a mass concentration of about 90% NH_3, Húsavík with 82% [9], while the Makatec's cooling process only uses 25% and 50% in its cycle.

The aim of this study is a thermodynamic comparison between the KSC-34 and the KC SG-1. The analysis includes a detailed review of zeotropic mixtures (NH_3/H_2O) as working fluid in a thermal process, as well as thermodynamic calculations based on energy and mass balance equations. In order to make the cycles comparable, boundary conditions for the heat source, heat sink and the efficiency of the auxiliaries are defined. Due to the different NH_3 concentrations used in the geothermal Kalina plants and the cooling cycle of Makatec's lab plant, each cycle is calculated for concentrations of 25%–100% of NH_3. The analysis focuses on the influence of the NH_3 concentration and the operation pressures. Cycle performances are compared based on their second law efficiencies.

2. The binary mixture NH_3/H_2O as working fluid

NH_3/H_2O is a so-called zeotropic mixture of two components with different boiling points leading to a sliding temperature profile during isobaric evaporation and condensation. At ambient pressure conditions the boiling point of NH_3 is 240 K, while the boiling point of H_2O 373.34 K. When a liquid NH_3/H_2O mixture is heated up to its boiling point, mainly NH_3 will start to evaporate reducing the fraction of NH_3 in the liquid, which leads to an increasing boiling temperature. When a gas is cooled to the dew point a higher amount of H_2O will condense, leaving an NH_3 enriched gaseous mixture with a lower dew point. The ratio between NH_3 and H_2O is an important factor impacting on the cycle and influences the following parameters:

- Evaporation temperature/pressure profile
- Condensation temperature/pressure profile
- Mass flow of the vapor in the turbine

The sound estimation of thermodynamic properties is a prerequisite when investigating these effects.

2.1. Properties of NH_3/H_2O mixtures

As basis for the calculation with NH_3/H_2O mixtures, knowledge of key thermo-physical properties of the mixture is required. These include thermodynamic properties (mainly enthalpy and entropy) and transport properties (mainly viscosity and thermal conductivity) of the fluid. Since NH_3/H_2O mixtures have been used in absorption heat pumps and refrigerators for years, the mixture is well known. However, for power cycle calculations, knowledge of the properties of NH_3/H_2O which are valid for higher pressures and temperatures are required.

In the simulation tool two alternatives for the calculation of the properties of NH_3/H_2O mixtures have been integrated. One is based on Ibrahim and Klein [14] and the other refers to the software REFPROP, version 9.0, of NIST [15] Using the equation of state of Tillner-Roth and Friend [16] for calculating the properties of NH_3/H_2O mixtures.

Fig. 1 presents in a T,ξ-diagram the comparison of saturation points calculated with the two alternative correlations. The lines depict the data of REFPROP and the dots are calculated result data of the Thermoflex software. The orange line represents the dew and bubble lines at 0.5 MPa, the blue line the dew and bubble lines at a higher pressure of 2 MPa.

According to [17] both estimates differ slightly. As presented in Fig. 1 the difference occurs mainly in the gas phase at an NH_3 mass fraction above 90%. Since calculations using the REFPROP formulation are time consuming, the following calculations are done with the correlations based on Ibrahim and Klein.

2.2. Thermodynamic characteristics of NH_3/H_2O

The isobaric phase change the mixture NH_3/H_2O occurs non-isothermally and mostly non-linear. The temperature profile during evaporation or condensation of NH_3/H_2O mixtures with different mass fractions and the pure fluids are presented in Fig. 2 in a T,h-diagram at a constant pressure of 2 MPa.

The non-linear behavior of the sliding temperature profiles of evaporating mixtures in the graph is not only valid for the presented pressure of 2 MPa and has an impact on the exergetic losses during heat transfer. In comparison, pure fluids have a constant temperature during phase change.

Unlike the isothermal phase change of pure fluid, this specific behavior of mixtures allows the process to take advantage of desorption and absorption characteristics [18]. The high and low process pressure level can be influenced in order to achieve optimal operating conditions. Figs. 3 and 4 demonstrate this phenomenon. Two NH_3/H_2O mixtures of 90% NH_3 and 93% are compared during evaporation and condensation. In an evaporator at a maximum process temperature of 393.15 K total evaporation of a 90% NH_3 mixture leads to a pressure of 1.5 MPa, while a 93% NH_3 mixture can totally evaporated at a higher pressure of 2 MPa. On the other hand,

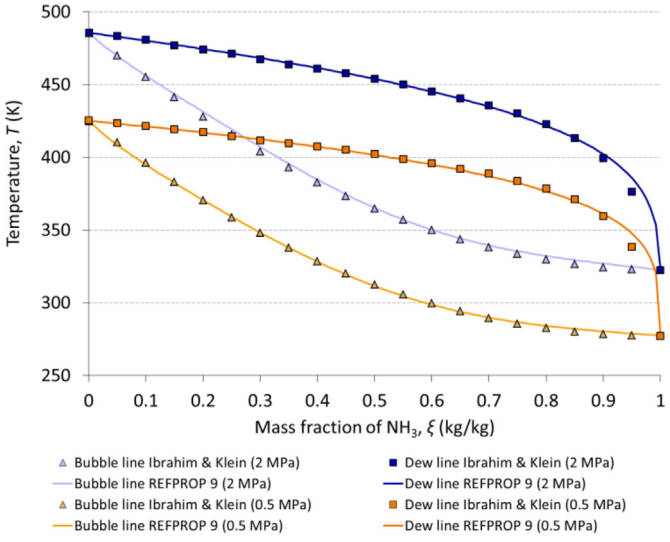

Fig. 1. Dew and bubble lines of the correlation of Ibrahim & Klein [14] and REFPROP 9 in comparison [15].

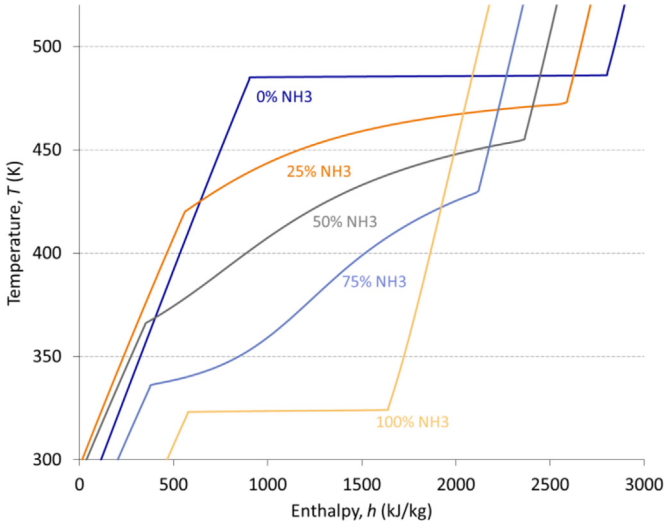

Fig. 2. Phase change of NH_3/H_2O mixture at different mass fraction ratio in a T,h-diagram at a constant pressure of 2 MPa [15].

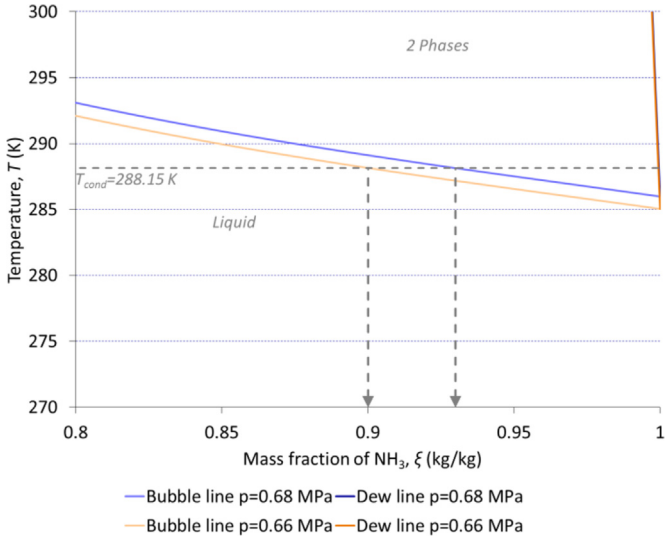

Fig. 4. Condensation conditions of two NH_3/H_2O mixtures (90% and 93% NH_3) [15].

the condensation of a gas with the higher 93% NH_3 mass fraction requires for a minimum temperature of 288.15 K a higher condensation pressure of 0.68 MPa compared to 0.66 MPa for the 90% NH_3 (Fig. 4). The higher mass fraction leads to a higher pressure ratio, which is favorable for the specific turbine output power.

An alternative method during evaporation is to stop the heat supply before total evaporation. An example is illustrated in Fig. 5 for a pressure of 2 MPa and a maximum temperature of 393.15 K. At those operation conditions a fluid with i.e. 90%NH_3 total mass fraction has a gas composition of 93%NH_3 while the liquid part has an NH_3 content of only around 36%. Regarding the bubble line for a mixture with 90% NH_3 the initial evaporation temperature of that composition is about 327 K. Such processes are usually described as desorption instead of evaporation and absorption instead of condensation.

When applying desorption/absorption processes in cycles by using NH_3/H_2O mixtures, the separation of the vapor and liquid phase is required before the turbine. This leads to a reduction of the mass flow through the turbine but also to a higher enthalpy difference in the turbine compared to total evaporation. During condensation the liquid and the vapor part are mixed again leading to the initial composition.

3. The cycle simulation

The software 'Thermoflex' is used for the thermodynamic cycle simulation in this report. This software has been developed by Thermoflow, and allows the user to assemble a plant model by selecting from a database of component types. This fully-flexible program for heat balance modeling can handle a variety of different working fluids. The implemented equations of state are introduced in 2.1. The cycle calculations can be done in both design and off-design. For the following calculations only the design mode is used [17].

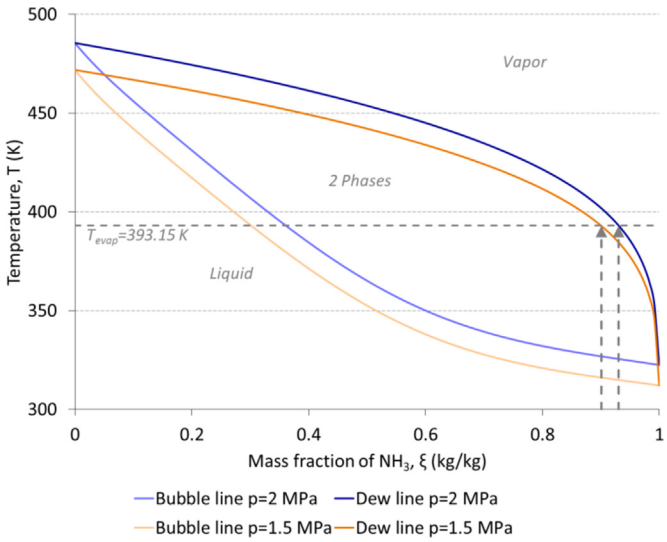

Fig. 3. Evaporation conditions of two NH_3/H_2O mixtures (90% and 93% NH_3) [15].

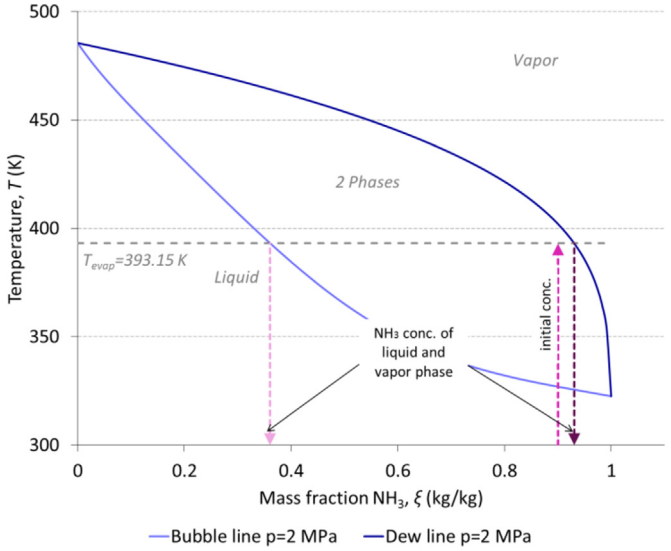

Fig. 5. Change of mass fraction of the liquid and vapor phase after separation [15].

3.1. Cycles in comparison

The Kalina technology is characterized by its binary working fluid. While the typical working fluid used in such a cycle is NH_3/H_2O, also other mixtures have been discussed in literature, including e.g. propane/hexane [19] or water/ethylene-glycol [20]. Therefore the cycle is not limited to the working fluid NH_3/H_2O, but it appears that only the NH_3/H_2O working fluid has been realized to date.

The cycle principle is similar to a regular ORC system. The working fluid evaporates at a high pressure level by the heat source. The produced steam enters a turbine to generate electricity. The expanded steam is condensed in an absorber. A pump raises the liquid back to the high pressure level before entering the desorber again. In most cases an internal heat exchanger complements the system, which recovers the heat from the hot exhaust of the turbine and preheats the condensate. In the analyzed NH_3/H_2O based cycles the mixture does not evaporate completely. Therefore a separator has to be installed to separate the liquid and vapor phase after desorption. Only the gas phase enters the turbine. To recover the heat as well from the hot liquid leaving the desorber the internal heat exchanger has a strong impact on the cycle efficiency. The basic flow sheets of the KC SG1 and KCS-34 that will be analyzed are shown in Fig. 6.

The difference between the two cycles compared is the position of the internal heat exchanger. While the KC SG1 recovers the heat of the expanded steam and the bypassed liquid, the KCS-34 recovers only the bypassed liquid. Therefore the KC SG1 recovers heat at a low system pressure leading to evaporation with temperature decrease for the liquid during pressure reduction while the KCS-34 internal heat exchanger works at high system pressure leading to a significant desorption of the liquid phase before entering the desorber.

3.2. Balance equations

In the cycle with the total mass fraction ξ_{cycle} and the total mass flow $\dot{m}_{cycle}$ the vapor and liquid phases are separated after the desorber. The related mass flows $\dot{m}_{vap}$ and $\dot{m}_{liq}$ at the outlet of the desorber are determined by the mass balances for a binary mixture in (1) and (2):

$$\dot{m}_{cycle} = \dot{m}_{vap} + \dot{m}_{liq} \tag{1}$$

$$\xi_{cycle} \cdot \dot{m}_{cycle} = \xi_{vap} \cdot \dot{m}_{vap} + \xi_{liq} \cdot \dot{m}_{liq} \tag{2}$$

Then the ratio between vapor and liquid mass flow can be calculated by (3):

$$\dot{m}_{vap} \Big/ \dot{m}_{liq} = \left(\xi_{cycle} - \xi_{liq}\right) \Big/ \left(\xi_{vap} - \xi_{cycle}\right) \tag{3}$$

The related internal turbine and pump work are calculated using isentropic efficiencies $\eta_{isentrop,Turbine}$ shown in (4) and (5) to correct the enthalpy differences during an isentropic expansion (turbine) or compression (pump).

$$W_{Turbine} = \eta_{isentrop,Turbine} \cdot \dot{m}_{vap} \cdot \Delta h_{Turbine} \tag{4}$$

$$W_{Pump} = \eta_{isentrop,Pump} \cdot \dot{m}_{cycle} \cdot \Delta h_{Pump} \tag{5}$$

For calculation of the net work of the process by (7), the external work for the cooling tower is required (6).

$$W_{CW} = W_{PumpCW} + W_{BlowerCT} \tag{6}$$

$$W_{Net} = W_{Turbine} - \left(W_{Pump} + W_{CW}\right) \tag{7}$$

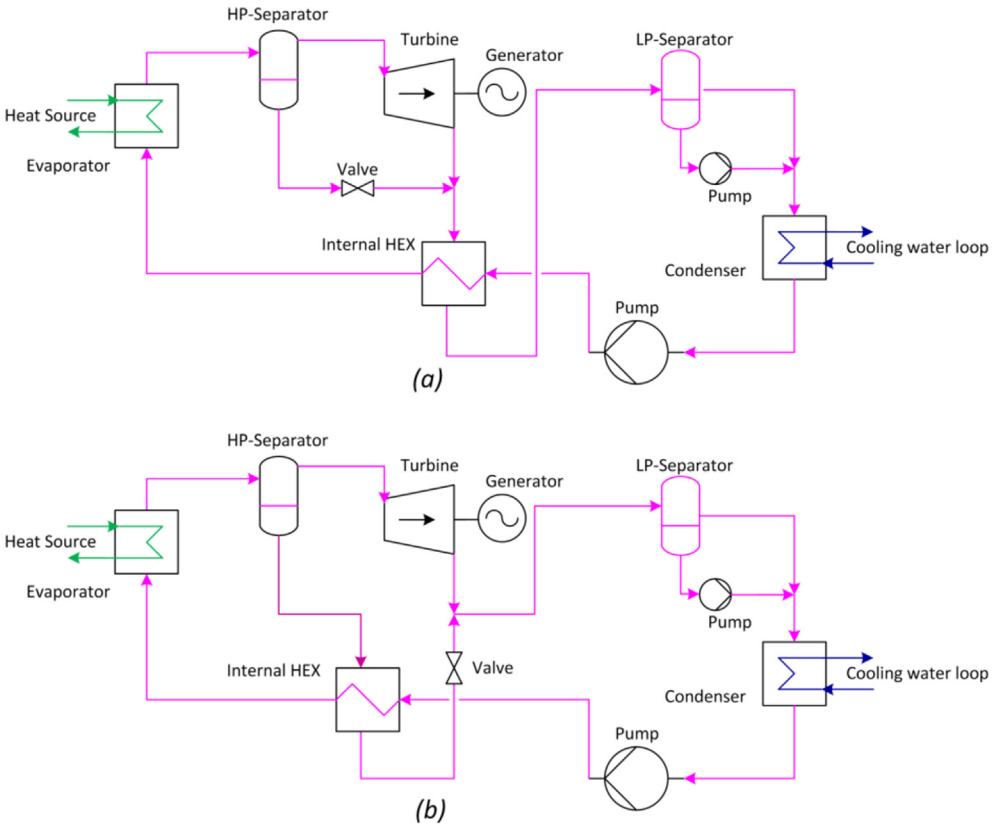

Fig. 6. Schematic plan of the KCS-34 (a) and the KC SG1 (b).

The exergetic efficiency is calculated as ratio of net work and exergy flow of the heat source with mass flow $\dot{m}_{HS}$ in (8).

$$\eta_{ex} = \frac{W_{Net}}{(h - h_0 - T_0 \cdot (s - s_0)) \cdot \dot{m}_{HS}} \quad (8)$$

The index 0 presents the reference point. In this case, the temperature T_0 is set to 288.15 K. The pressure is chosen according to the heat source pressure of 0.2 MPa.

3.3. Boundary conditions

The required boundary conditions for the cycle simulation are based on low temperature level waste heat sources from cement production. Boundary conditions are set for the heat source and ambient conditions as well as additional set values like pressure drops, pinch points and efficiencies. All assumptions are listed in Table 1.

4. Results and discussion

In this study, cycle performances have been simulated based on variations of the NH_3 mass fraction in a range from 25% to 100%. This is due to a wide spread in existing plants. Makatec's resorption process (KCS-34) for cooling uses 25% and 50% of NH_3 mass fraction, while EnBW's Kalina process (KC SG1) is operated between 80% and 90%.

4.1. Process optimization

The maximum net power output has been selected as the key criterion for optimization of the process. The optimization aims particularly at waste heat applications without any related cost for the heat, where it is a better criterion compared to energetic process efficiency. The work of the turbine has the largest impact on the net power output since the auxiliaries only fluctuate slightly depending on certain parameters of the cycle.

The basic conditions for optimization of the net power output by the maximum pressure (the pressure entering the turbine) at given initial total composition and desorber outlet temperature can be explained as follows. Choosing a maximum pressure determines the ratio $\dot{m}_{vap}/\dot{m}_{liq}$ at the desorber outlet. While the gas content of NH_3 increases with the increasing desorber outlet pressure (Fig. 3) the mass flow of the vapor decreases according to equation (3). The low pressure of the cycle at given composition is determined by the cooling water temperature and pinch point in the absorber and does not depend on the maximum pressure for a given total composition. The turbine work can then be calculated with the other relevant boundaries for this total composition and desorber pressure outlet. The optimization is illustrated in Fig. 7 for the KCS-34 with a mixture of 50% NH_3.

Table 1
Boundary conditions assumed for the cycle comparison.

Heat source	Temperature T_{HS}	368.15 K
	Mass flow $\dot{m}_{HS}$	1 kg/s
	Pressure p_{HS}	0.2 MPa
Heat exchanger	Minimal Pinch ΔT_{PP}	3 K
	Pressure drops in HEX Δp_{HEX}	0.02 MPa
	No sub-cooling at absorber ΔT_{sub}	0 K
Cooling tower	Wet cooling tower with mechanical draft	
	Ambient temperature $T_{ambient}$	291.15 K
	Wet bulb temperature T_{wb}	286.15 K
	Fan efficiency η_{fan}	0.6
	Air draft loss $\Delta p_{CT,air}$	0.3 kPa
	Pressure drop CT (water side) Δp_{CT}	0.025 MPa
	Pressure drop water cycle Δp_{CW}	0.025 MPa
	Cooling water approach to wet bulb temperature ΔT_{CT}	5 K
Turbine	Isentropic efficiency $\eta_{Turbine}$	0.8
Pump	Isentropic efficiency η_{Pump}	0.75

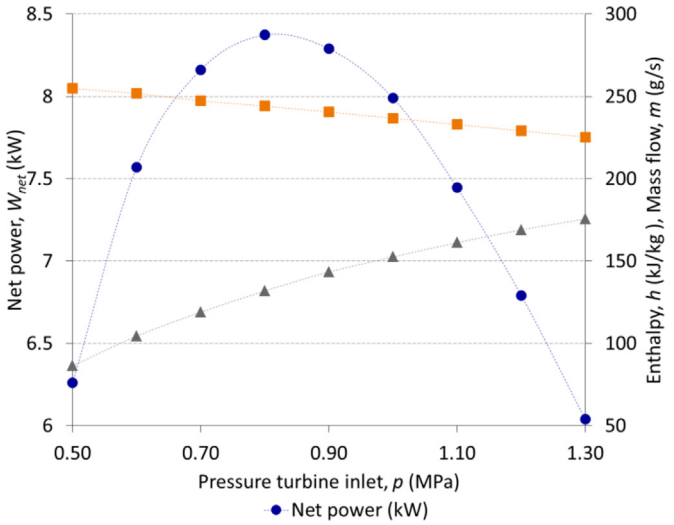

Fig. 7. Optimization of net power output by the high pressure of the cycle, here KCS-34 at 50% NH_3.

Fig. 7 shows that the optimum of the high system pressure is in the range of 0.8 MPa for the mixture used in this example. Since the increasing enthalpy difference with increasing pressure is related to a decreasing vapor mass flow, an optimum pressure can be determined for all compositions.

4.2. The influence of the internal heat exchanger

The optimum pressures for different initial compositions of the mixtures in the KCS-34 and the KC SG1 are presented in Fig. 8. The low optimal pressure level of the cycle depends on the cooling conditions. Therefore this pressure is always equal for the KCS-34 and the KC SG1 when NH_3 mass fraction is at the same level.

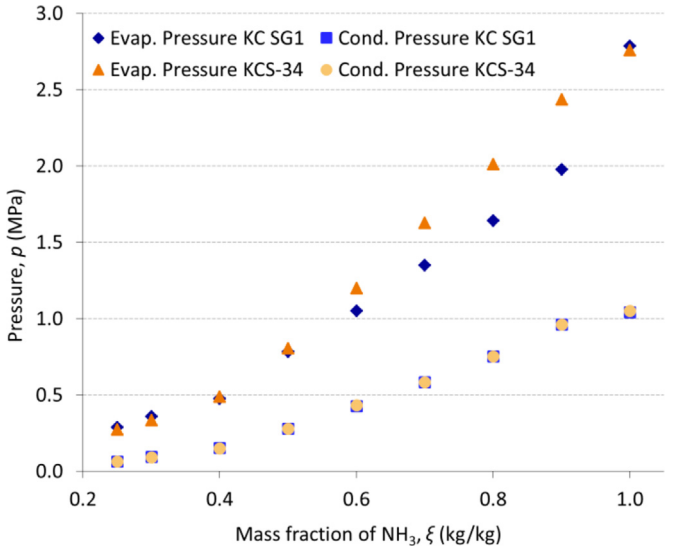

Fig. 8. High and low pressure of the KC SG1 and KCS-34 depend on the NH_3 mass fraction.

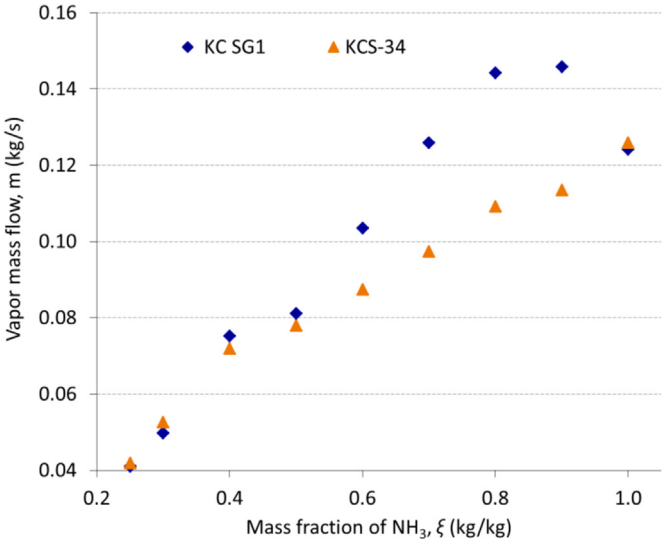

Fig. 9. Vapor mass fraction in comparison: KC SG1 and KCS-34 depend on the NH_3 mass fraction.

Also, both the high and the low pressure increase in line with NH_3, which is in accordance with the basic equilibrium conditions.

The high system pressure differs between the two cycles. At a NH_3 mass fraction between 60% and 90% the high pressure of the KCS-34 in Fig. 8 shows higher pressures compared to the KC SG1.

The observation that the KC SG1 can run with lower pressures compared to the KCS-34 is also stated in the Siemens patent [12] and is confirmed by the results of the process calculations for high NH_3 concentrations. Due to the lower high pressure of the KC SG1 compared to the KCS-34, the evaporation temperature of the working fluid is lower. At an equal evaporation temperature, the KC SG1 has the advantage to evaporate higher amounts of working fluid, leading to an increase of the vapor mass flow compared to the KCS-34 as shown in Fig. 9.

Two main factors influence the cycle's net power output: a high enthalpy difference and a high vapor mass flow through the turbine.

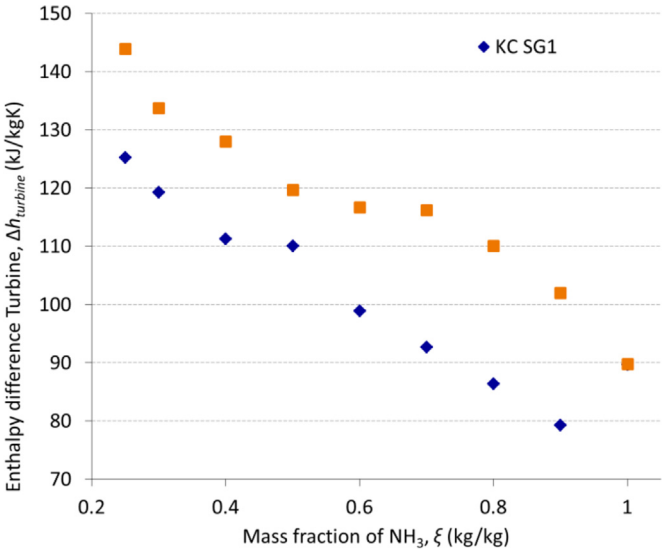

Fig. 10. Enthalpy difference at the turbine of the KC SG1 and KCS-34 depend on the NH_3 mass fraction.

While in the KC-SG1 the mass flow through the turbine is higher, the KSC-34 benefits from a higher pressure difference at the turbine. This is illustrated by the enthalpy difference at the turbine in Fig. 10. The enthalpy difference of the cycle configuration KSC-34 is about 11%–22% higher depending on the NH_3 mass fraction.

Being the only difference in the process design, these effects must be caused by the internal heat exchangers of both cycles. While the KC SG1 recovers also the expanded vapor after the turbine, the KCS-34 only uses the by passed liquid for heat recovery. As illustrated in Fig. 11, for a 70% NH_3 mixture at optimized conditions the internal heat exchange of the KC SG1 is significantly higher than for the KCS-34.

Looking at the internal heat exchanger of the KCS-34 in more detail, it becomes apparent that for high initial NH_3 concentrations the large temperature difference between the hot solutions is due to a relatively low mass flow of the liquid leaving the hot desorber. Therefore, the concept of the KC SG1 leads to a better performance of the internal heat exchange because a relevant fraction of the mixture is evaporated. Fig. 12 shows the energy flow of each cycle component at NH_3 mass fractions of 30% and 70%. While the liquid–liquid internal heat exchanger of the KCS-34 recovers a higher amount of energy at the low NH_3 mass fraction, the internal heat exchanger of KC SG1 shows better performance at the high NH_3 mass fraction.

The KCS-34's internal heat exchanger is in the bypass of the turbine and does not affect the pressure of the turbine outlet, while for KC SG1 the pressure drop of the internal heat exchanger increases the pressure after the turbine. This also has an impact on the cycle performance. However, at high mass fractions the optimum of the high pressure must be increased for the KCS-34 compared to the KC SG1. For mass fractions below 50% the impacts of both effects compensate each other leading to the same pressure range for both cycles. As visualized in Fig. 12, the amount of heat transferred from the heat source to the working fluid varies between the cycles. Despite the lower heat load at the evaporator of the KCS-34, the work of the turbine is higher compared to the KC SG1 at low NH_3 concentrations. On the contrary, turbine performance is slightly better for KC SG1 at higher NH_3 concentrations.

4.3. Exergy analysis

For waste heat applications the maximization of the net work output is equivalent to the optimum of the exergetic efficiency, also called second law efficiency. In Fig. 13 the exergetic efficiency is illustrated for the comparison of KCS-34 and KC SG1. Furthermore a pure fluid ORC's performance is shown for reference. As working fluid for the ORC without internal heat exchanger R245fa is considered. R245fa is an often analyzed and applied refrigerant in ORC systems because of its environmentally-friendly characteristic [21]. The maximal exergetic efficiency is reached at an NH_3 mass fraction of 80% for the KC SG1 and the KCS-34. A slightly better maximum exergetic efficiency of 27% is reached by the KC SG1. As mentioned above, the difference can be explained by the better performance of the internal heat exchanger. Compared to the ORC the exergetic efficiency can be increased by the KC SG1 of almost 25%. At lower mass fractions of NH_3 the KCS-34 has a better performance, because the ratio $\dot{m}_{vap}/\dot{m}_{liq}$ decreases leading to a better performance of the liquid–liquid internal heat exchanger. This region can be of interest for applications if the maximum temperature spread for the heat source is limited.

Furthermore the cycle operates on a lower high pressure level compared to optimum efficiency conditions. Then requirements regarding the material and safety can be reduced.

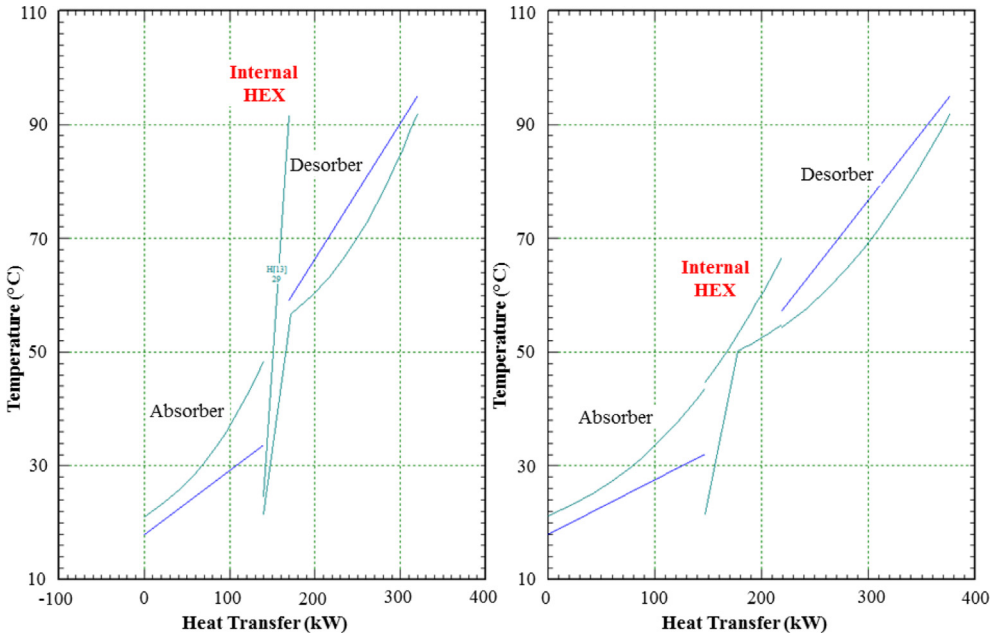

Fig. 11. Heat transfer of absorber, internal heat exchanger and desorber of the KCS-34 (left) and KC SG1 (right) cycles at a mass fraction of 70% NH_3 [17].

5. Conclusion and final remarks

Thermodynamic calculations suggest that the application of NH_3/H_2O mixtures as working fluid in binary cycles can lead to a significant increase in the efficiency of power generation from low enthalpy source. For the selected heat source of 393.15 K (hot water) the optimal NH_3 mass fraction that reaches the best performance has been found to be between 80% and 90%. Compared to an ORC using R245fa as working fluid, the exergetic efficiency can be increased by the NH_3/H_2O based cycles by approximately 25%. Here, the KC SG1 achieves a slightly better performance compared to the KCS-34.

The key difference between the KC SG1 and the KCS-34 lies within the internal heat exchanger. It has an influence on the vapor mass flow and on the enthalpy difference of the turbine. While the KC SG1 reaches a higher mass flow through the turbine, the KCS-34 operates at a higher enthalpy difference at the turbine.

This increase in efficiency could not be verified through actual plant operations, yet [22]. Both the KC SG1 in Bruchsal and the KCS-34 of Makatec face challenges. These are mainly associated with the absorption and resorption process, where technical issues still need to be overcome in order to achieve theoretical performance potentials. Especially the design of a reliable absorption process with small amounts of liquid compared to the amount of gas is not yet solved. Optimum performance is theoretically achieved at those conditions. Furthermore, the use of NH_3/H_2O as working fluid requires specific material selection in order to mitigate the risk of damages through corrosion [23].

If all NH_3/H_2O related challenges can be solved in the future, this mixture appears to be a promising environmentally friendly and

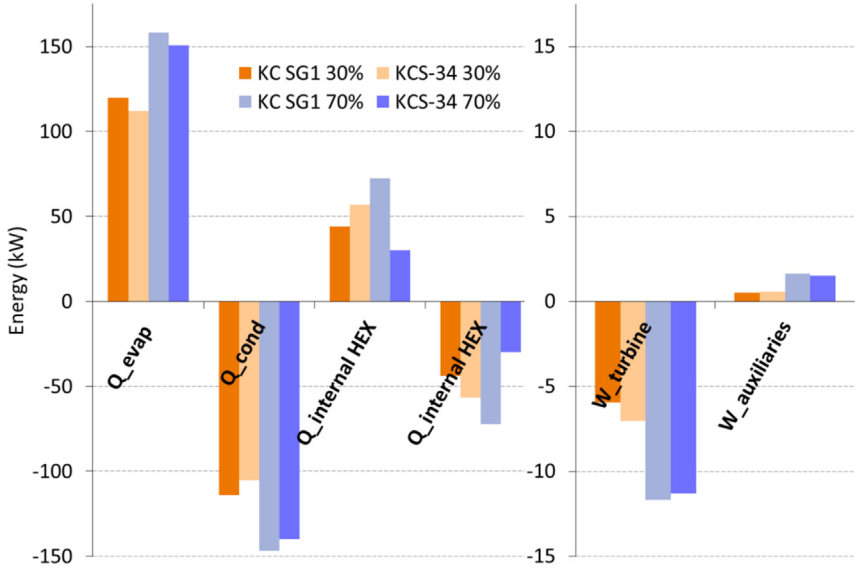

Fig. 12. Energy flow of each component of the cycles in comparison: KC SG1 and KCS-34 at 30 and 70% of NH_3 mass fraction.

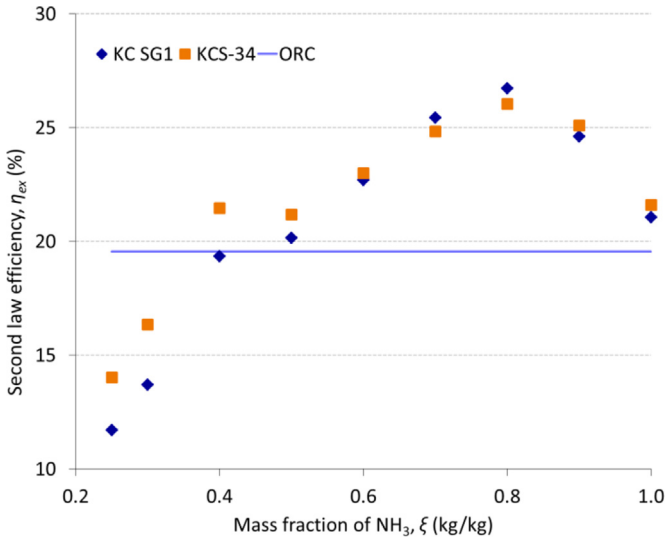

Fig. 13. Exergetic efficiency of the KC SG1, KCS-34 and ORC in comparison.

efficient alternative for power generation from low-temperature heat sources.

The theoretical analysis of NH_3/H_2O based cycles is ongoing. Further research will focus on a more detailed validation of the simulation results of the KC SG1 and KCS-34 with the goal to establish an economic and high efficient process that can be implemented in practice.

Acknowledgments

The research leading to these results has received funding from the European Community's Seventh Framework Program (FP7/2007-2013) under grant agreement n 256790 ('LOVE').

Nomenclature

h	enthalpy (kJ/kg)
H_2O	water
HP	high pressure
LP	low pressure
$\dot{m}$	mass flow rate (kg/s)
NH_3	ammonia
p	pressure (MPa)
s	entropy (kJ/s)
T	temperature (K)
W	work (kW)

Greek letters

Δ	difference
η	efficiency
ξ	mass fraction (kg/kg)

Subscripts

0	reference point
cond	condenser/absorber
CT	cooling tower
CW	cooling water
evap	evaporator/desorber
ex	exergetic
HEX	heat exchanger
HS	heat source
in	inlet
isentrop	isentropic
liq	liquid
out	outlet
PP	pinch point
sub	subcooling
vap	vapor
wb	wet bulb

Acronyms

KC SG	Kalina cycle system geothermal
KCS	Kalina cycle system
ORC	Organic Rankine cycle

References

[1] Ogriseck S. Integration of Kalina cycle in a combined heat and power plant, a case study. Appl Therm Eng 2009;29:2843–8.
[2] Wang J, Dai Y, Gao L. Exergy analyses and parametric optimizations for different cogeneration power plants in cement industry. Appl Energy 2009;86:941–8.
[3] Zahoransky RA, Allelein HJ, Bollin E, Oehler H, Schelling U, Schwarz H. Energietechnik Systeme zur Energieumwandlung: kompaktwissen für Studium und Beruf. In: Zahoransky R, editor. Geothermie. Wiesbaden, Germany: Springer Fachmedien; 2013. p. 360–77.
[4] Valdimarsson P. ORC and Kalina. Analysis and experience. 2003. Available at: http://www.sero.se/Filer/Husavik.pdf [accessed 25.01.13].
[5] Lolos PA, Rogdakis ED. A Kalina cycle driven by renewable energy sources. Energy 2009;34:457–64.
[6] Kalex Systems. Kalex LLC. Superior efficincy, reducing costs, viable alternative energy. 2010. Available at: http://kalexsystems.com/ [accessed 02.03.15].
[7] Zhang X, He M, Zhang Y. A review of research on the Kalina cycle. Renew Sustain Energy Rev 2012;16:5309–18.
[8] Kalina A., Method and apparatus of converting heat to useful energy. European patent application. Date of patent: Jan.2001.
[9] MlCak H., Mirolli M., Hjartarson H., Ralph M., Notes from the North: a report on the debut year of the 2 MW Kalina Cycle® geothermal power plant in Húsavík, Iceland.
[10] Knapek E, Kittl G. Unterhaching power plant and overall system. In: Proceedings european geothermal Congress; 2007.
[11] Mergner H, Eggeling E, Kölbel T, Münch W, Genter A. Geothermische Stromerzeugung Bruchsal und Soutlz-sous-Forêts. 20. In: Symposium Felsmechanik und Tunnelbau. Mining & Geo; 2012.
[12] Lengert, J., Verfahren und Vorrichtung zur Ausführung eines thermodynamischen Kreisprozesses. Europäische Patentschrift EP 1613841 B1. Date of patent: Dec.2006.
[13] Bundesverband geothermie, Kalina prozess. Available at: http://www.geothermie.de/wissenswelt/glossar-lexikon/k/kalina-prozess.html [acessed 02.03.15].
[14] Ibrahim O. M., Klein, S. A., Thermodynamic properties of ammonia-water mixtures, ASHRAE Trans CH-93-21-2, pp. 1495–1502.
[15] NIST, NIST Reference Fluid Thermodynamic and Transport Properties - REFPROP 9.0. National Institute of Standards and Technology, Boulder, Colorado, U.S. Department of Commerce.
[16] Tillner-Roth R, Friend DG. A helmholtz free energy formulation of the thermodynamic properties of the mixture {water + ammonia}. J Phys Chem Reference Data 1998;27(1):63–96.
[17] Thermoflow Inc, Thermoflex Version 23, Southborough, Massachusetts, USA.
[18] Gicquel R. Energy systems: a new approach to engineering thermodynamics. Leiden, Netherland: CRC Press; 2012.
[19] Vijayaraghavan S. Thermodynamic studies on alternative binary working fluid combinations and configurations for a combined power and cooling cycle [dissertation]. Florida, USA: University of Florida; 2003.
[20] Bajorek SM, Schnelle J. identification and experimental database for binary and multicomponent mixtures with potential for increasing overall cycle efficiency. Manhattan, USA: Kansas State University, Department of Mechanical and Nuclear Engineering; 2002 May. Final Report DOE Award No.: DE-FG26–99FT40589.
[21] Kang SH. Design and experimental study of ORC (organic Rankine cycle) and radial turbine using R245fa working fluid. Energy 2012;41:514–24.
[22] DiPippo R. Second law assessment of binary plants generating power from low-temperature geothermal fluids. Geothermics 2004;33:565–86.
[23] Whittaker P. Corrosion in the Kalina cycle. An investigation into corrosion problems at the Kalina cycle geothermal power plant in Húsavík, Iceland [master thesis]. Akureyri, Iceland: University of Iceland & University of Akureyri; 2009.